

# Exergetic study of catalytic steam reforming of bio-ethanol over Pd–Rh/CeO<sub>2</sub> with hydrogen purification in a membrane reactor

Ali Hedayati, Institute of Energy Technologies, Universitat Politècnica de Catalunya, Diagonal 647, 08028 Barcelona, Spain, [ali.hedayati@upc.edu](mailto:ali.hedayati@upc.edu)

Olivier Le Corre, Department of Energy Systems and Environment, Ecole des Mines de Nantes, 4 rue A. Kastler, 44307 Nantes, France, [Olivier.LeCorre@mines-nantes.fr](mailto:Olivier.LeCorre@mines-nantes.fr)

Bruno Lacarrière, Department of Energy Systems and Environment, Ecole des Mines de Nantes, 4 rue A. Kastler, 44307 Nantes, France, [bruno.lacarriere@mines-nantes.fr](mailto:bruno.lacarriere@mines-nantes.fr)

Jordi Llorca, Institute of Energy Technologies, Universitat Politècnica de Catalunya, Diagonal 647, 08028 Barcelona, Spain, [jordi.llerca@upc.edu](mailto:jordi.llerca@upc.edu)

## Abstract

In this work, we present the application of exergy analysis in the evaluation of the ethanol steam reforming (ESR) process in a catalytic membrane reactor (CMR) containing Pd-Ag membranes sandwiched by Pd-Rh/CeO<sub>2</sub> catalyst to produce fuel cell grade pure hydrogen (no sweep gas). ESR experiments were performed at T=873-923 K and P=4-12 bar. The fuel was a mixture of ethanol and distilled water with steam to carbon ratio=1.6, 2, and 3. The exergy evaluation of the system is based on the experimental data, where total yields of 3.5 mol H<sub>2</sub> permeated per mol ethanol in feed with maximum hydrogen recuperation of 90% were measured at 923 K and 12 bar. The exergy efficiency of the system was evaluated considering both the insulated reactor (without heat loss), and non-insulated reactor (with heat loss). Exergy efficiency up to around 50% was reached in the case of the insulated reactor at 12 bar and 923 K. It was concluded that the highest amount of exergy was destructed by heat losses. The study showed that the exergy content of the retentate gas can provide the reactor with a notable fraction of its required heat at steady state conditions which can remarkably increase the overall exergy efficiency of the system. In this case, thermal efficiency of the insulated reactor was between 70-90%, which decreased to 40-60% when the heat loss was considered.

Keywords: exergy, hydrogen, catalytic membrane reactor, ethanol steam reforming

## Highlights

- Ethanol steam reforming experiments were performed in a membrane reactor
- Hydrogen yield of 0.55 and hydrogen recovery 92% were obtained
- 0.9 L<sub>N</sub> pure hydrogen per ml of converted ethanol was produced
- Exergy efficiency up to 50% was calculated in the case of an insulated reactor
- Reactor insulation and retentate gas exergy recovery increased the efficiency of the system are the key factors for system optimization
- Heat losses are the main source of exergy loss
- The retentate gas has a large amount of recoverable exergy content

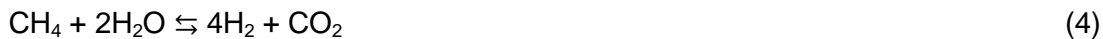
## 1. Introduction

As an alternative to fossil fuels, hydrogen is considered as a clean energy carrier that can be combusted similar to the conventional carbonaceous fuels or converted to electricity by fuel cells [1]. The use of renewable biofuels such as bio-ethanol as a source of hydrogen is highly beneficial

due to the higher H/C ratio, lower volatility and toxicity, and higher safety of storage that distinguishes ethanol over other substrates. Bio-ethanol is cheaply and easily obtained from biomass and organic waste and can be used directly in catalytic steam reforming processes to produce hydrogen since it contains large amounts of water [2]. Among the reforming processes, steam reforming of bio-ethanol (eq. 1) delivers the highest amount of hydrogen per mole of converted bio-ethanol [3].



Huge amount of works has been reported in the literature on catalytic ethanol steam reforming (ESR) specially on the experiential investigations aiming for hydrogen generation using a variety of catalysts in different reactor configurations [4–8]. The distinctive properties of noble metals such as high activity, hindering carbon from depositing on the catalyst active sites, and durability and robustness during the ESR process have attracted the attention of a lot of research groups toward such catalysts [9,10]. Further, the formation of undesired chemical species is minor or zero when noble metal based catalysts are used for the ESR process [6,9]. Based on this fact, in this work we have used a Pd-Rh/CeO<sub>2</sub> catalyst and CH<sub>4</sub>, CO<sub>2</sub>, CO and H<sub>2</sub> have been the only products of the ESR experiments, which are obtained via following reaction pathways [10,11]:



Equations 2 to 4 represent ethanol decomposition, water gas shift reaction, and methane steam reforming reactions, respectively. The importance of understanding the main products is obvious when the exergy content of each stream is taken into account. Therefore, the only species present in the inlet and outlet streams are H<sub>2</sub>O, C<sub>2</sub>H<sub>5</sub>OH, CH<sub>4</sub>, CO<sub>2</sub>, CO, and H<sub>2</sub>. The experiments were performed in a membrane reactor with selective Pd-based metallic membranes for producing pure hydrogen in which the production and separation of hydrogen took place simultaneously. The benefits of catalytic membrane reactors (CMRs) such as simultaneous generation and separation of hydrogen, cost reduction, simplicity of the design, and reforming reactions promotion beyond the equilibrium limits (the shift effect) are well known and repeatedly reported in the literature [12–15].

According to the open literature, there are a few reported studies on exergetic efficiency evaluation of ethanol steam reforming systems for hydrogen production. The term exergy is defined as the maximum work that can be obtained theoretically from a system interacting with the source environment to equilibrium [16]. Exergy differs from energy in the way that energy is conserved, but exergy can be dissipated. Despite the first law of thermodynamics – which states the conservation of energy - exergy is defined based on the second law of thermodynamics stating that it is not possible to fully utilize the thermal energy as we stay in atmospheric conditions [17]. In other words, exergy is the ability of available energy to convert into other forms of energy. Hence, exergy can be conserved only if the process between the environment and the system is reversible [18].

Taking into account the second law of thermodynamics, exergy is derived from the entropy, free energy (Helmholtz energy), and Gibbs free energy (free enthalpy). Therefore, exergy is a function of the thermodynamic state of the substance under study and the reference environment [17]. In

the light of exergy definition, it can be understood that the main difference between energy (thermal) efficiency and exergy efficiency lies in the consideration of the thermodynamic state of every single component, which results in an exact understanding of the available amount of work, together with the unavoidable irreversibility during a process. Considering the conservation of mass and energy together, exergy analysis is a powerful tool to investigate the imperfections of single components of the system to obtain a clearer understanding of the local irreversibility. This also makes it possible to study the effect of thermodynamic factors on the performance of an energy system to decide on the most favorable operational conditions in terms of process efficiency and energy usage [19,20].

As reported in the literature, Kalinci et al. [21] studied the production of hydrogen via a gasification-boiler system based on experimental data taken from the literature using different types of biomass. They found the maximum exergy efficiency to be about 12%. An exergy analysis based on chemical exergy on biological hydrogen production from biomass was done by Modarresi et al. [22], who reported exergetic efficiencies of 36-45%, depending on the process configuration. The thermochemical water splitting process for hydrogen production via the Cu-Cl cycle was investigated by Orhan et al. [23] and Joshi et al. [24] modelled the exergy of different methods of solar hydrogen production. For reforming processes, Simpson et al. [1] modelled the methane steam reforming process and both irreversible chemical reactions and heat losses were identified as the main source of exergy destruction, whereas exhaust gases contained large amounts of chemical exergy. Casas-Ledón et al. [18] studied hydrogen production from ESR considering based on the first and the second law of thermodynamics. They evaluated the exergy efficiency of the system at different operational conditions (pressure, temperature, and S/C ratio) considering the unused and destructed exergy during the ESR process. They concluded that the exergetic efficiency of the ESR system was a function of temperature and S/C ratio, while no effect of pressure on exergy efficiency was observed. A comprehensive exergy analysis of the different types of ethanol reforming processes (ESR, POX and ATR) based on a model in Aspen Plus was performed by Khila et al. [19]. The same formulation as Casas-Ledón et al. [18] was used by Khila et al. and they calculated the exergy of the inlet and outlet streams at selected operational conditions, according to hydrogen production per mole of inlet ethanol. An exergy efficiency of 70% was claimed for the ESR process, considering total hydrogen production via ESR as the main product. In another interesting study, Tippawan et al [25] employed the first and second law of thermodynamics to evaluate energy and exergy performance of an modelled ethanol reforming system in connection with a solid oxide fuel cell (SOFC) with a similar formulation as Casas-Ledón et al. [18] and Khila et al [19]. They studied ESR, partial oxidation (POX), and autothermal reforming (ATR) processes as the reforming sections for hydrogen production, and the best efficiency of the system (reforming+SOFC) was stated equal to 60% when ESR was used as the reformer unit. Finally, Hedayati et al. [26] reported exergetic evaluation of the ESR process in a staged membrane reactor based on experimental results. They considered only pure hydrogen as the desired product. It was reported that a big share of exergy is destroyed due to the irreversibility of reforming reactions and heat losses.

In this work, we present energy and exergy analysis of the ESR process in a catalytic membrane reactor (CMR) containing Pd-Ag membranes sandwiched by Pd-Rh/CeO<sub>2</sub> catalyst to produce pure hydrogen (no sweep gas). The exergy evaluation of the system is based on the experimental data, where total yields of 3.5 mol H<sub>2</sub> permeated per mol ethanol in feed with maximum hydrogen recuperation of 90% were measured, which are outstanding results compared to what has been reported in the literature [27,28]. The novelty of this work lies in the application of exergy analysis

to evaluate the ESR process in a packed bed CMR configuration based on experimental results and observations. As the area of the membrane science and pure hydrogen production in the membrane reactors is growing, exergetic evaluation of the CMR systems – as the first essential step for system analysis via exergetic optimization – can open a new chapter in this science to approach larger scale applications.

## 2. Material and methods

### 2.1. Experimental

The Pd-Rh/CeO<sub>2</sub> catalyst (0.5% Pd–0.5% Rh) was deposited over cordierite pellets of about 1-3 mm following the procedure described by López et al. [27]. The laboratory setup used for the ESR experiments (fuel reformer) consisted essentially of a fuel tank, a liquid pump, a CMR, a pressure transducer and a condenser. A detailed description of the reformer setup can be found in [26]. The commercial CMR (provided by Reb Research) was 10 in. tall and 1 in. in diameter. There were four Pd-Ag membrane tubes selective to hydrogen inside the reactor; each one 3 in. tall and 1/8 in. diameter in order to separate hydrogen from the gases produced. The reactor was filled with the catalysts so that the metallic membranes were covered. The scheme of the CMR is presented in Fig. 1.

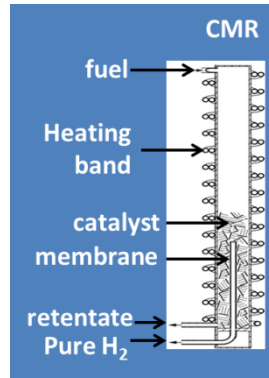


Fig. 1: Scheme of the catalytic membrane reactor (CMR)

The operating conditions of the experiments are summarized in table 1.

Table 1: Experimental conditions

Temperature (K)	873-923
Pressure (bar)	4 – 12
Fuel flow rate (μl/min)	50 – 100
S/C	1.6 – 3

The pure hydrogen production rate is considered as the main point of evaluation of the CMR system. Factors such as hydrogen yield ( $Y_{H_2}$ ) and hydrogen recovery ( $R_{H_2}$ ) were selected to evaluate the performance of the CMR.

$$Y_{H_2} = \frac{F_{H_2.perm}}{6 \times F_{EtOH}} \quad (5)$$

$$R_{H_2} = \frac{F_{H_2.perm}}{F_{H_2.total}} \quad (6)$$

Where  $F_{H_2, \text{perm}}$ ,  $F_{EtOH}$ , and  $F_{H_2, \text{total}}$  are pure hydrogen permeation flow rate, ethanol flow rate, and total hydrogen production, respectively, in mol/s. Total hydrogen production includes the permeated hydrogen and the hydrogen content of the retentate gas. The molar flow rates of  $CH_4$ ,  $CO_2$ ,  $CO$ , and not permeated  $H_2$  in the retentate stream (waste gas) were calculated using the chromatographic analyses and the volumetric flow rates of the retentate.  $F_{H_2, \text{perm}}$  was directly measured by a mass flow meter Bronkhorst xxx(model).

## 2.2. Exergy analysis

The traditional method of process performance evaluation based on the first law of thermodynamics is performed according to the lower heating value (LHV) of the inlet and outlet streams, plus the amount of work or heat provided to run the process. Thermal efficiency of the reformer system is defined as [19,26]:

$$\eta_{Thermal} = \frac{\sum \dot{m}_{gas} \times LHV_{Products}}{\dot{m}_{EtOH} \times LHV_{EtOH} + \dot{w}_{pump} + \dot{Q}} \quad (7)$$

Where  $\dot{Q}$  represents the heat losses, the required heat for evaporation and heating the fuel (reactants) up to the reaction temperature, plus the required heat for the reforming reactions. Heat losses account for the heat released to the environment through the reactor wall, products cooling down, and water condensation. The reactor wall was considered as a stainless steel cylinder, transferring heat to the reference environment. To calculate the heat loss at different operating conditions, reactor wall temperature (in contact with air) was measured by means of a thermocouple. The required heat for the evaporation and heating up the reactants was calculated according to the fuel flow rate and S/C ratio of each experiment. The heat required for the reforming reactions also was calculated based on the progress of each of the reaction (eq. 2-4) using the retentate composition.

Exergy efficiency is a function of exergy destruction and unused exergy. This formulation has been repetitively used by different researchers [18,19,26,29]. Exergy destruction is defined as:

$$E_{x\text{destruction}} = EX_{in} - EX_{out} \quad (8)$$

Where  $EX_{in}$  and  $EX_{out}$  are the exergy flows of the inlet and outlet streams. Therefore,  $EX_{in}$  represents the exergy of inlet fuel (water+ethanol) plus the required heat for the ESR process (including heat losses), and  $EX_{out}$  denotes the pure hydrogen stream (permeate side) plus the retentate gases exiting the reactor. The condensed water is considered to have zero exergy value. The unused exergy is calculated as:

$$EX_{unused} = EX_{destruction} + EX_{retentate} \quad (9)$$

Where  $EX_{retentate}$  is equal to the exergy content of the retentate gas. In this work, the useful part of exergy is considered as the exergy of the pure hydrogen stream. Accordingly, the fraction of hydrogen in the retentate gas (not permeated fraction) is not taken into account as the main product. Finally, the exergy efficiency of the ESR process is given by equation 8:

$$\eta_{ex} = 1 - \frac{EX_{unused}}{EX_{in}} \quad (10)$$

The exergy content of the mass flow of each specie (i) in each stream includes physical exergy, chemical exergy, and mixing exergy were taken into account:

$$EX_i = EX_{physical} + EX_{chemical} + EX_{mixing} \quad (11)$$

Physical exergy ( $EX_{physical}$ ) is the maximum obtainable work produced when a stream is brought from the actual conditions ( $T, P$ ) to the reference conditions ( $P_0, T_0$ ) by a reversible process and is defined as [18,30] :

$$EX_{physical} = h - h_0 - T_0(S - S_0) \quad (12)$$

$h$  and  $S$  are the enthalpy and entropy of the substance at actual (reaction) conditions, and  $h_0$  and  $S_0$  are the enthalpy and entropy of the substance at reference conditions, respectively. The dependency of the physical exergy on enthalpy and entropy demonstrates two advantages. First, exergy is a function of the state of the matter, and second, each matter is considered independently in a stream, not as a mixture. Both advantages result in a more precise idea on the performance of a thermal system. In this work, the reference temperature and pressure are defined as  $T_0 = 298.15$  K and  $P_0 = 1.013$  bar. To calculate the values of enthalpy and entropy, NASA polynomials (Chemkin polynomial coefficients) [31,32] for temperatures below 1000 K were applied.

Chemical exergy originates from the difference between the chemical potentials when a substance is changed at reference conditions to the chemical equilibrium state with the concentrations of components. In this work, the chemical exergy of each specie was calculated using the standard chemical exergy table given by Bejan model II [16]. Chemical exergy occasionally is reported as a sum of two terms, i.e. the standard chemical exergy plus a logarithmic term as a function of the fraction of each substance in a mixture [18,25]:

$$EX_{chem} = \sum_i x_i \varepsilon_i + RT_0 \sum_i x_i \ln x_i \quad (13)$$

Where  $x_i$  is the fraction of specie  $i$  in the mixture of gases,  $\varepsilon_i$  is the standard chemical exergy of the same species, and  $R$  is the universal gas constant. The second term, as is always negative, can be ascribed to the exergy of mixing. Exergy of mixing is the entropy generated when pure substances are mixed and is given by equation 12 [17]:

$$EX_{mix_i} = x_i RT_0 \ln x_i \quad (14)$$

Hence, the mixing process is irreversible and exergy of mixing is always negative. However, the value of mixing exergy is normally negligible in front of standard chemical exergy [30]. A comprehensive discussion on various types of exergy calculation is given by Sato [17] and Hinderink et al. [30]. Similar definitions have been reported in some studies which are based on the entropy difference between the mixture of substances and the pure components (which exist in the mixture) individually [19,30]. In this work, all three types of exergy were considered for each species in the inlet and outlet streams. The molar flow rate of reactants and products obtained during the experimental work were used for evaluation of the exergy flow of each stream.

### 2.3. System under study

It is assumed that the reactants enter the system at reference conditions and products are released to the same environment. The scheme of the system under study is shown in Fig. 2.

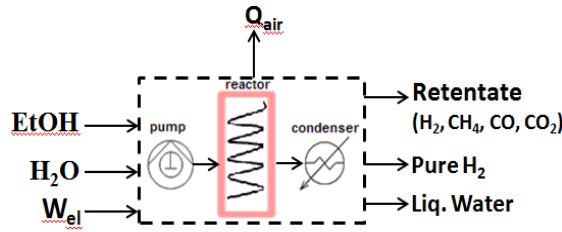


Fig. 2: Scheme of the boundary of the reformer system

$Q_{air}$  represents the heat loss. In fact, this heat in the form of exergy is a part of the inlet exergy stream ( $W_{el}$ ) which is released to the environment as unused exergy.  $W_{el}$  represents the electrical input of the system used by the heating band to provide the reactor with required heating. In this study,  $W_{el}$  is replaced by the required heat for the ESR process, which will be equal to the term ' $\dot{Q}$ ' in equation 5. The work of the pump is neglected in exergy and energy evaluations.

### 3. Results and discussion

#### 3.1. Experimental results

Both hydrogen production and its permeation through the membrane depend on temperature. On one hand, hydrogen permeation through the membrane is a temperature activated phenomena and, on the other, hand the progress of methane steam reforming (MSR) as the dominant hydrogen producing reaction is favored naturally with temperature as it is an endothermic chemical reaction (eq. 3). This behavior is shown in Fig. 3 at constant S/C ratio and fuel flow rate (FF) for two temperatures, 873 and 923 K.

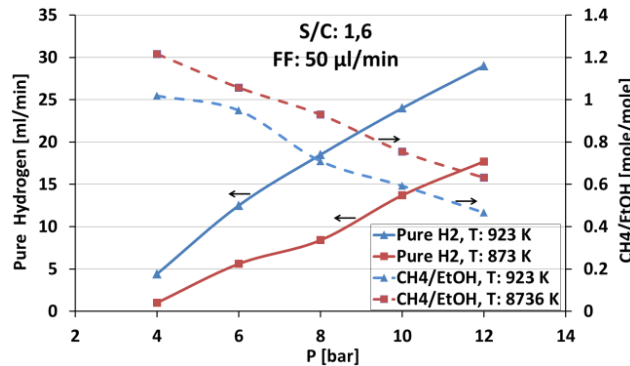


Fig. 3: Effect of temperature and pressure on the permeated hydrogen and on the methane production ratio. FF represents the fuel flow rate in µl/min.

Pure hydrogen production gets doubled as the temperature increases by 50 K from 873 K to 923 K, at constant S/C ratio and fuel flow rate and  $P > 6$  bar. At  $P < 6$  bar, traces of methanation are seen ( $\frac{\text{mole CH}_4}{\text{mole EtOH}} > 1$ ). This phenomenon is caused by operating at high pressure where the MSR reaction (eq. 3) is pushed backward according to Le Chatelier's Principle. At pressures greater than 6 bar, hydrogen permeation is improved as a result of higher partial pressure of hydrogen around the membrane (Sieverts' law). Therefore, MSR and WGS reactions are promoted, as the catalyst is available around the membrane to compensate for the removed product (permeated hydrogen). This is an evident result of the shift effect in CMR configuration leading to the promotion of the reforming reactions. In the light of the shift effect, it is obvious that as more methane is converted, more hydrogen is produced and therefore permeated as pure hydrogen. Temperatures lower than

873 K were not tested because the permeation of hydrogen (pure hydrogen production) was neglectable.

Hydrogen permeation at two different fuel flow rates is shown in Fig. 4. At higher pressures the gap between the two flow rates is widened as a result of higher rates of hydrogen permeation through the membrane. It is proved that the catalyst around the membrane is able to compensate for the permeating hydrogen by simultaneous hydrogen production. As more hydrogen is permeated, more hydrogen is produced via ESR due to the shift effect especially at higher pressures. Therefore, in case of availability of more fuel, relatively more hydrogen is permeated.

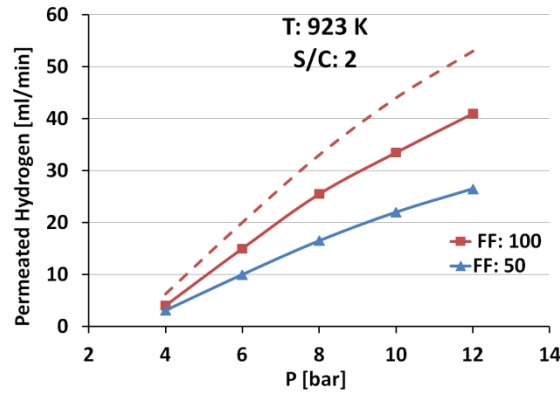


Fig. 4: Effect of fuel flow rate (FF) on pure hydrogen flow rate. FF represents the fuel flow rate in  $\mu\text{l/min}$ .

The dashed line illustrates the expected permeation rate of hydrogen at FF=100  $\mu\text{l/min}$  which is equal to the doubled amount of the pure hydrogen flow rate at FF=50  $\mu\text{l/min}$ . The reason why this value is not reached lies in the fact that not all the converted hydrogen can permeate through the membrane while the inlet ethanol is doubled.

As stated by Sieverts' law, the driving force for pure hydrogen permeation through a membrane is proportional to the partial pressure of hydrogen in the retentate side (around the membrane). The higher is the operating pressure, the higher is the partial pressure of hydrogen around the membrane. In other words, the special configuration of the reactor resulted in overcoming the negative effect of pressure on the reforming reaction due to the nature of the reactions (Le Chatelier's Principle).

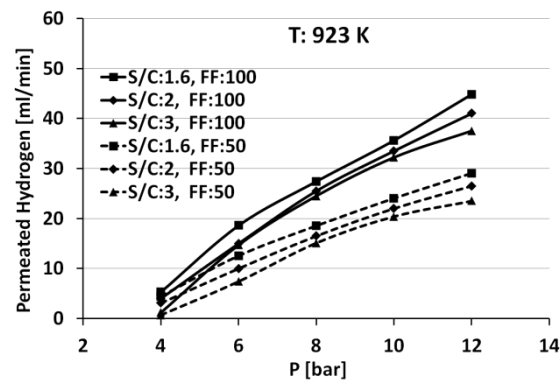


Fig. 5: Pure hydrogen production at different fuel flow rates and S/C ratios. FF represents the fuel flow rate in  $\mu\text{l/min}$ .



Figure 5 shows the results concerning the effect of the S/C ratio. The pure hydrogen flow rate declines with S/C ratio because less ethanol as the source of hydrogen is fed into the CMR at higher S/C ratios and because the excess water results in a lower hydrogen partial pressure inside the reactor. Pressures higher than 12 bar and temperatures higher than 923 K were not tested because of the experimental setup limitations.

Hydrogen yield is a well-known indicator of the performance of hydrogen producing systems. According to equation 5, hydrogen yield refers to pure hydrogen, which can reach up to 1 if 6 moles of pure hydrogen are obtained and permeated through the membrane per 1 mole of inlet ethanol (ideal conditions, i.e. complete conversion of ethanol to  $\text{CO}_2$  and  $\text{H}_2$ ).

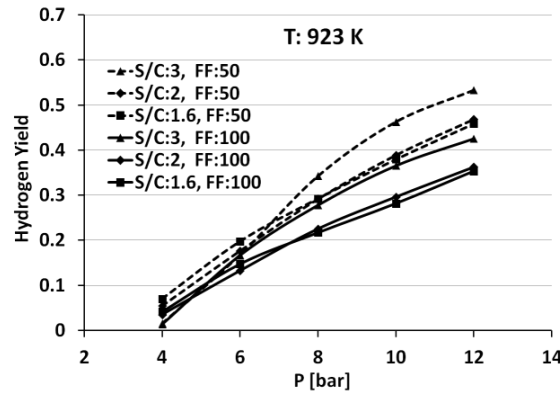


Fig. 6: Hydrogen yield obtained at different fuel flow rates and S/C ratios. FF represents the fuel flow rate in  $\mu\text{l}/\text{min}$ .

According to the Sieverts' law, hydrogen yield increases with pressure (Figure 6). An increase of the S/C ratio results in a higher hydrogen yield due to lower molar flow rate of ethanol in the feed.

At complete ethanol conversion, hydrogen recovery is a measure of the ability of the system to produce pure hydrogen. This refers essentially to the membrane performance and obviously high values are required due to the high cost of the Pd-Ag membranes. The hydrogen recovery as a function of pressure is presented in Fig. 7.

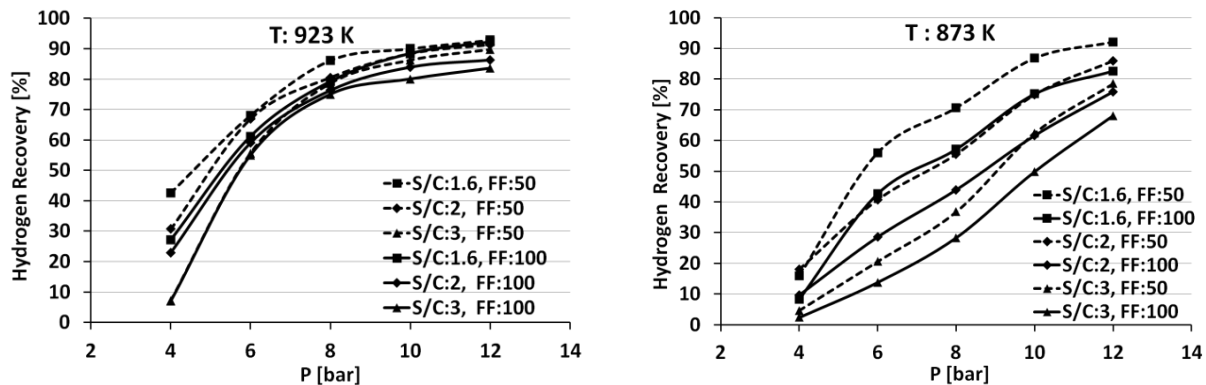


Fig. 7: Hydrogen recovery at different experimental conditions. FF represents the fuel flow rate in  $\mu\text{l}/\text{min}$ .

As expected, hydrogen recovery is favored at lower S/C values since the partial pressure of hydrogen in the reactor is higher (less excess water) and, hence, the permeation through the membrane is improved according to Sieverts' law. In addition, at a lower fuel flow rate the contact time increases and the permeation of hydrogen is favored. At 923 K, hydrogen recovery increases

sharply up to 8 bar and after that the trend becomes less sharp which is due to the hydrogen fraction in the retentate side. However, at pressures greater than 8 bar, the thermodynamics are unfavorable to the reforming reactions resulting in almost constant partial pressure of hydrogen inside the reactor. On average, for every 2 bar increase in pressure, the pure hydrogen production increases by 0.5 mole/mole ethanol in the feed. Accordingly, the fraction of hydrogen in the retentate side decreases with pressure, which is attributed to the fact that more hydrogen is permeated (recovered) through the membrane. Pure hydrogen production rate and hydrogen fraction in the retentate side as a function of pressure are illustrated in Fig. 8.

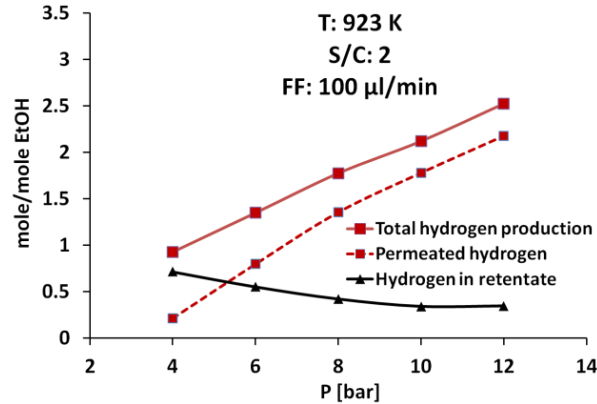


Fig. 8: Hydrogen flow rate in different streams. FF represents the fuel flow rate in  $\mu\text{l}/\text{min}$ .

## 3.2. Exergy evaluation results

### 3.2.1. Effect of operational conditions on exergy efficiency

Pressure has a strong effect on exergy efficiency. As seen in Fig. 9, the best exergy efficiency is obtained at 12 bar, whatever the temperature.

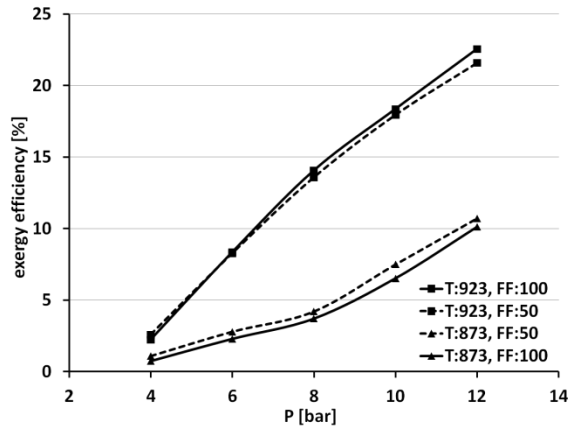


Fig. 9: Effect of pressure on exergy efficiency at 873-923 K and S/C = 2. FF represents the fuel flow rate in  $\mu\text{l}/\text{min}$ .

Following the pure hydrogen permeation rate (Fig. 5), the highest exergy efficiency is reached at the highest pressure, which is in agreement with hydrogen production and hydrogen yield.

The effect of temperature is seen in Fig. 10. At 873 K the system is not efficient, even at high pressure. This is ascribed to the important role of methane steam reforming (MSR) reaction, which

produces the highest number of moles of. This clearly demonstrates the importance of high temperature to reform methane and run the system efficiently. The effect of the fuel flow rate of the exergy efficiency is not noticeable.

The composition of the inlet fuel – which is stated by steam to carbon ratio (S/C) – showed different effects on the reforming system at 873 and 923 K. The exergy efficiency increased slightly with the S/C ratio at 923 K, while an opposite effect was seen at 873 K (Fig. 10).

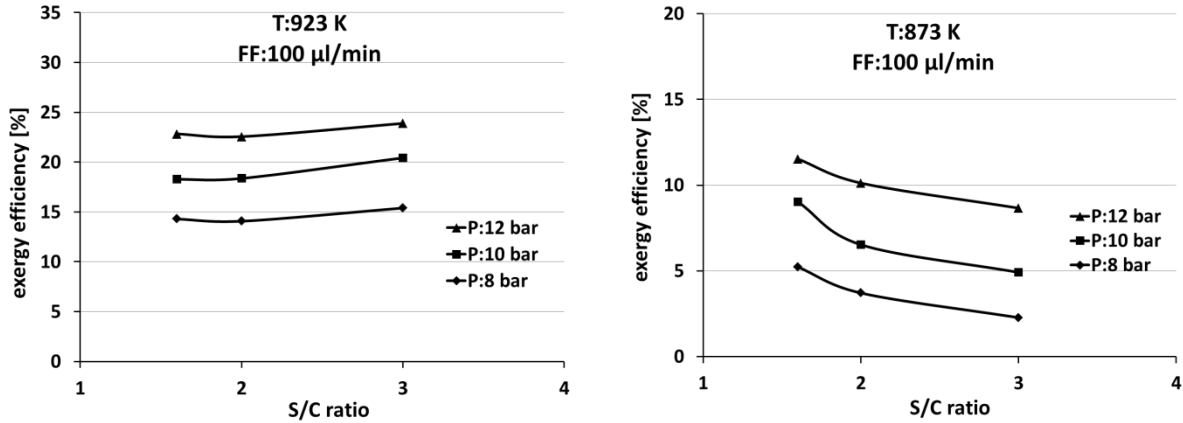


Fig. 10: Effect of S/C ratio on exergy efficiency

The effect of S/C ratio at each temperature is explained considering the molar production rate of pure hydrogen per mole ethanol in the feed. At complete conversion of ethanol, the governing reforming reaction determines the hydrogen production rate and therefore the value and the trend of exergy efficiency as a function of the S/C ratio. At 873 K, the water gas shift (WGS) reaction is dominant because it is favored at lower temperatures. At a lower S/C ratio more ethanol is fed into the system and more CO is formed to be used in the WGS reaction. Accordingly, more hydrogen is produced at lower S/C ratio. On the contrary, at 923 K, the MSR reaction is favored as a higher amount of water is available (higher S/C) and more hydrogen is produced.

The comparatively lower values of the exergy efficiency obtained in this work in comparison with what has been reported in the literature [19,20,25] are explained by taking into account that here we only consider the exergy content of pure hydrogen as the evaluation base (not the total hydrogen produced).

### 3.2.2. Exergy efficiency improvement

#### 3.2.2.1. Exergy flows

Analysis of the exergy content of each inlet/outlet stream leads to obtain a better understanding of the performance of the system and the feasibility to recover or decrease the exhaust or destructed exergy. The exergy destruction due to the irreversibility attributable to the reforming reactions lessens with S/C ratio because there is less ethanol in the feed. Heat loss constitutes one of the major shares of exergy destruction accounting for 50% of the outlet exergy flow on average at FF=50 µl/min. Another notable source of exergy loss is the retentate gas, which contains CH<sub>4</sub>, CO, and not permeated H<sub>2</sub>. According to the evaluation, there is a considerable amount of exergy in the retentate gas that could be used for the ESR process. Since the system best performance was achieved at 923 K and 12 bar, the analysis of the system in terms of inlet/outlet exergy flows was

done at these conditions. Figure 11 shows the comparison between the inlet and outlet exergy flows calculated at 923 K and 12 bar under different fuel flow rates and S/C ratios. As can be seen, the major source of exergy loss is related to heat loss and retentate gases. Therefore, the exergy efficiency of the reforming system can be improved by insulation of the reactor and recovery of the retentate gas exergy content.

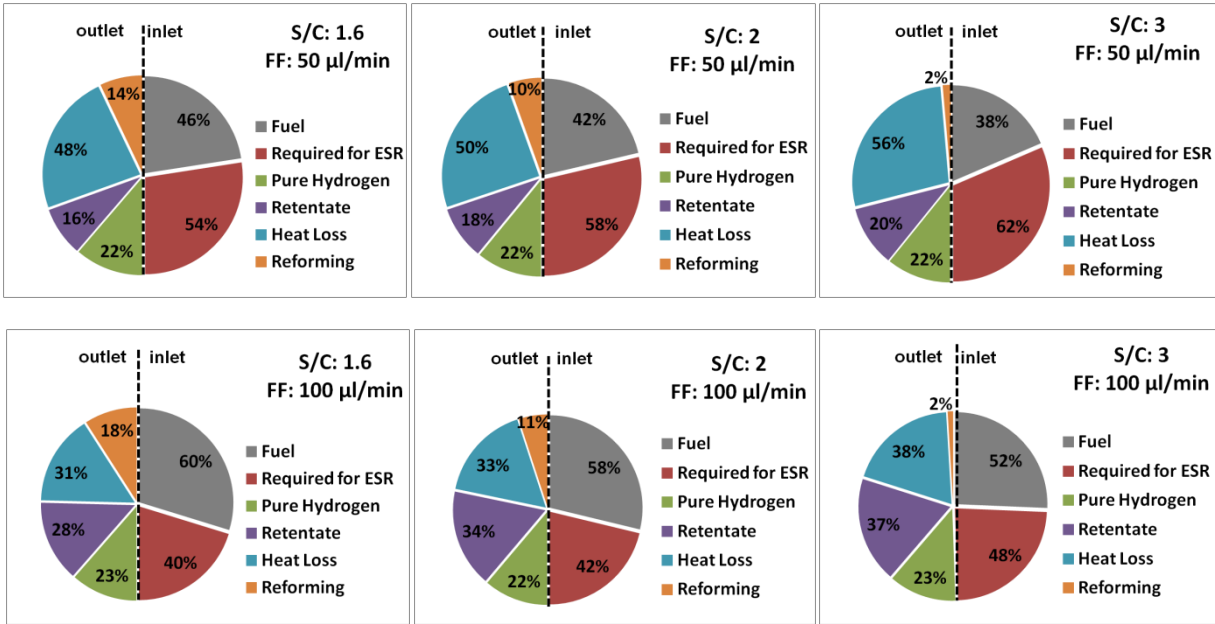
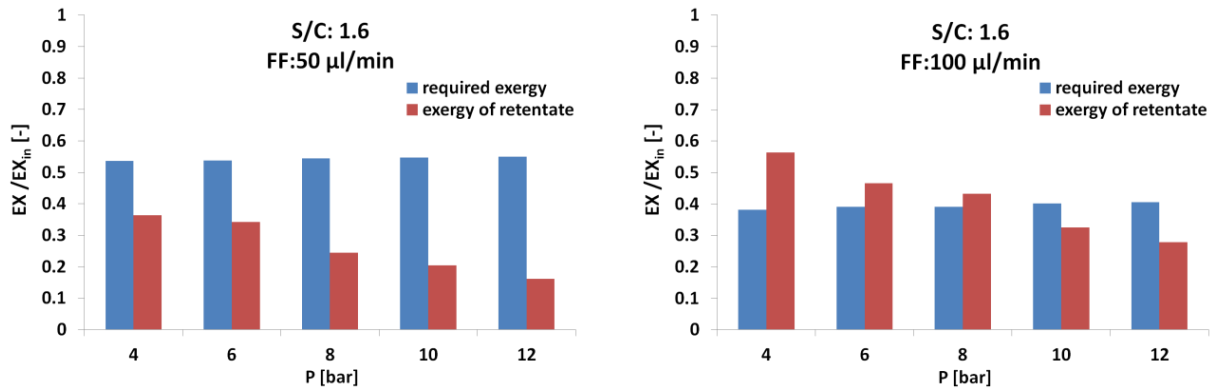


Fig. 11: Exergy flows at 923 K and 12 bar at various S/C ratios. FF represents the fuel flow rate in  $\mu\text{l/min}$ .

### 3.2.2.2. Recovery of the retentate gas stream

The combustion of the retentate gas is a clear source of energy to provide the required heat for the ESR reactor. In Fig. 12, the ratios of the exergy content of the retentate gas and the required exergy to the inlet exergy ( $EX_{in}$ ) at 923 K are shown.



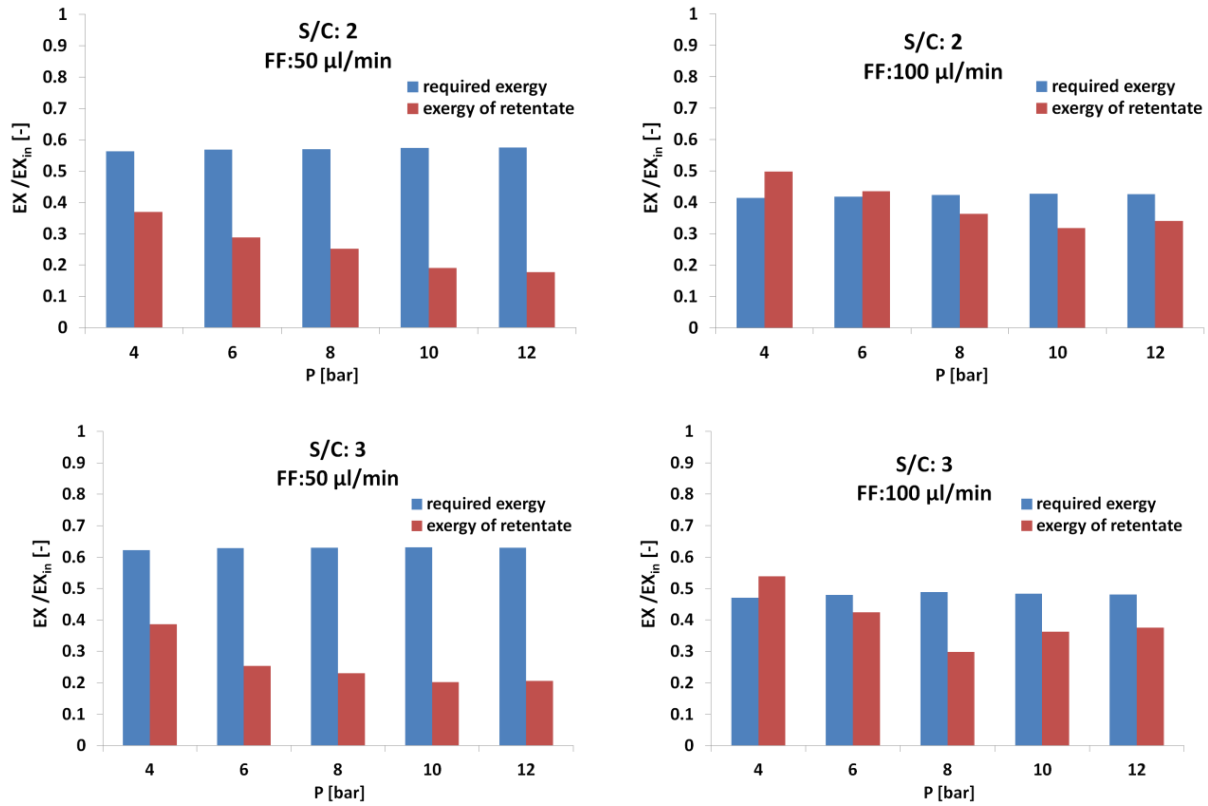


Fig. 12: Exergy of the retentate gas and required exergy vs. pressure for the ESR process at  $T = 923$

The exergy content of the retentate gas is high enough to provide the reactor with a notable fraction (at  $FF=50 \mu\text{l/min}$ ) or all (at  $FF=100 \mu\text{l/min}$ ) of its required energy at steady state conditions. The exergy content of the retentate gas is significantly higher at  $FF=100 \mu\text{l/min}$  due to the high molar production rate of methane. Hence, the exergy efficiency is improved as the value of  $W_{el}$  is reduced (see Fig. 2) so that at  $923 \text{ K}$ ,  $12 \text{ bar}$ ,  $S/C=3$ , and  $FF=100 \mu\text{l/min}$ , the exergy efficiency increases by 14% (absolute value). The comparison between the values of exergy efficiency in case of utilization of the retentate gas at  $923 \text{ K}$  and  $12 \text{ bar}$  and different  $S/C$  ratios is presented in table 2.

Table 2: comparison of exergy efficiency in case of retentate gas utilization at  $T = 923 \text{ K}$  and  $P = 12 \text{ bar}$

FF [ $\mu\text{l/min}$ ]	50			100		
S/C ratio	1.6	2	3	1.6	2	3
Exergy efficiency [%] - retentate not used	22.3	21.6	21.3	22.8	22.6	23.9
Exergy efficiency [%] - retentate used	26.7	26.2	26.9	31.6	34.2	38.2

### 3.2.2.3. Insulated reactor

In case of an insulated reactor ( $Q_{air} \rightarrow 0$ ), the exergy efficiency is remarkably improved. In order to calculate the heat loss rate, the reactor external wall temperature was measured by means of a thermocouple when the system was operating in steady state conditions. If the reactor is insulated,

the energy demand of the system is limited to the heat needed to run the system at a certain temperature. This heat is used for fuel evaporation and heating up to reaction temperature, and the reforming reactions. The exergy efficiency of the insulated system at similar conditions as in Fig.9 is illustrated in Fig. 13.

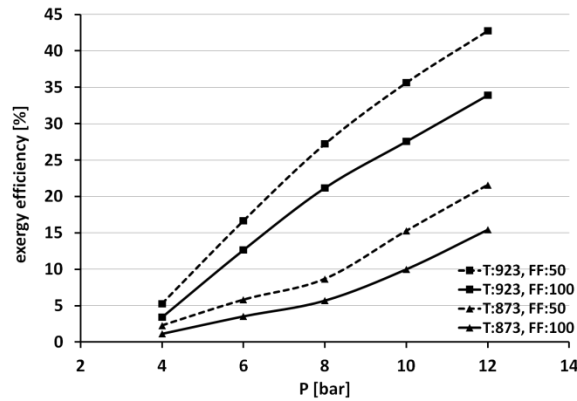


Fig. 13: Effect of pressure on exergy efficiency at 873-923 K, FF = 50-100  $\mu\text{l}/\text{min}$ , and S/C = 2 for the insulated reactor

At pressures higher than 8 bar, and especially at 923 K the exergy efficiency is highly improved. In the case of the insulated reactor, the effect of the fuel flow rate is more obvious (see Fig. 3) which is attributed to the dominant effect of heat losses when the reactor is not insulated. Exergy efficiency is higher at FF = 50  $\mu\text{l}/\text{min}$  because the pure hydrogen production rate does not double when the fuel flow rate does, as discussed above. The dependency of exergy efficiency on S/C ratio is clearer in an insulated reactor due to the dominant value of ethanol exergy in the inlet stream. The concentration of ethanol in the feed is lower at higher S/C ratio. The exergy efficiency of the insulated reactor system is presented in table 3.

Table 3: Exergy efficiency at P = 12 bar and  $F_F = 50 \mu\text{l}/\text{min}$  for the insulated reactor

T [K]	873			923		
S/C ratio	1.6	2	3	1.6	2	3
Exergy efficiency [%]	26.2	21.6	17.6	42.1	42.8	47.7

Following the trend of exergy efficiency, unused exergy is an obvious function of temperature and pressure when an insulated reactor is considered. The reason lies in the rate of pure hydrogen production and the presence of methane as the major component of the retentate stream in terms of exergy content. Methane production per mole of inlet ethanol decreases by 50% as pressure increases from 4 bar to 12 bar at S/C = 1.6 (see Fig.3). At higher pressure, as less methane appears in the retentate stream, the exergy content of retentate is greatly decreased. The rate of unused exergy compared to inlet exergy ( $EX_{in}$ ) at different operating conditions is given in Fig. 14.

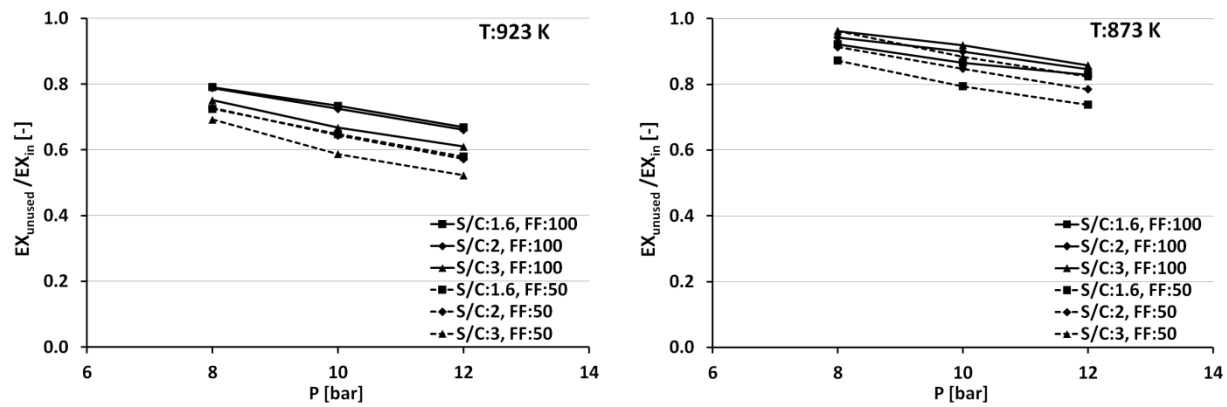


Fig. 14: Unused exergy for the insulated reactor. FF represents the fuel flow rate in  $\mu\text{l/min}$ .

At  $P < 8$  bar, hydrogen permeation rate is very low, resulting in huge amounts of reformed gases leaving the reactor as retentate stream. Hence, a huge share of inlet exergy is lost in the form of unused exergy (see eq. 7).

By utilization of the retentate gas in an insulated reactor, the exergy efficiency is increased drastically and is placed between 70-90 %, which is a high value compared to the reported works in the literature, bearing in mind that permeated pure hydrogen is considered as the only product of the reforming system. This result is expected since in one hand exergy destruction decreases and on the other hand the energy requirement of the system is partially or totally met by utilization of the retentate gas, which is usefulness in terms of obtaining a pure hydrogen stream.

### 3.2.3. Thermal efficiency

Thermal efficiency is calculated based on the energy conservation principle, not taking into account the utilizable part of the energy and quality change of energy during an irreversible process (see eq. 5). In this way, thermal efficiency is normally higher than exergy efficiency. Thermal efficiency of the studied system at  $T = 923$  K and  $P = 12$  bar is given in table 4.

Tabled 4: Thermal efficiency at  $T=923$  K and  $P=12$  bar

$F_F$ [ $\mu\text{l/min}$ ]	50			100		
S/C ratio	1.6	2	3	1.6	2	3
Thermal efficiency [%] - non isolated system	38	38	38	50	55	57
Thermal efficiency [%] - isolated system	74	78	89	74	84	96

Thermal efficiency is a combination of two factors, i.e. the rate of hydrogen production and the flow rate and composition of the retentate gas since the retentate flow contains large amount of methane with a high LHV. The main difference between thermal efficiency and exergy efficiency of the ESR systems is that while thermal efficiency offers an ideal performance at high pressure and temperature, exergy efficiency discloses inevitable irreversibility even when the reactor is insulated. The pressure has no significant effect on the thermal efficiency; instead, S/C ratio is the determining factor. On the contrary, when considering exergy efficiency, it is possible to

understand and relate the pure hydrogen production rate as a function of pressure, which is in agreement with the Sieverts' law.



#### 4. Conclusion

ESR experiments over Pd-Rh/CeO<sub>2</sub> were performed in a CMR containing Pd-Ag separation membranes using ethanol and water mixtures at different S/C ratios. Hydrogen yield of 0.55 and hydrogen recovery of 90% were reached as a result of the special configuration of the CMR. More than 0.9 L<sub>N</sub> of pure hydrogen permeated per ml ethanol in fuel at 12 bar and 923 K were obtained. An exergetic analysis was performed based on these experimental results aiming not only to evaluate the performance of the CMR system, but also to introduce the application of the exergy analysis in CMRs studies. Both insulated and non-insulated reactor systems were evaluated in terms of exergy destruction, exergy efficiency, and thermal efficiency. The effects of pressure and temperature were dominant and the study showed that the system reached around 50% exergy efficiency at 923 K and 12 bar in an insulated reactor. Unused exergy decreased with pressure since the MSR reaction is promoted at high pressures in CMRs as more hydrogen is permeated due to the availability of the catalyst around the membrane and the shift effect. It was concluded that the retentate gas exergy content can compensate the energy requirements of the reactor in steady state and improve the exergy efficiency significantly. The highest exergy destruction occurred via heat losses and the retentate stream. The thermal efficiency of the process was also evaluated based on the LHV of ethanol and the products and compared to the exergy efficiency to explain the advantages of using exergy evaluation in a CMR.

#### Acknowledgments

Funding from MINECO project ENE2012-36368 is acknowledged. Ali Hedayati gratefully acknowledges Erasmus Mundus Joint Doctoral Program SELECT+. Jordi Llorca is Serra Húnter Fellow and is grateful to ICREA Academia program.

#### References

- [1]  Simpson, A. Lutz, Exergy analysis of hydrogen production via steam methane reforming, International Journal of Hydrogen Energy. 32 (2007) 4811–4820. doi:10.1016/j.ijhydene.2007.08.025.
- [2] G.  Deluga, J.R. Salge, L.D. Schmidt, X.E. Verykios, Renewable hydrogen from ethanol by autothermal reforming., Science (New York, NY). 303 (2004) 993–997. doi:10.1126/science.1093045.
- [3] G. Rabenstein, V. Hacker, Hydrogen for fuel cells from ethanol by steam-reforming, partial-oxidation and combined auto-thermal reforming: A thermodynamic analysis, Journal of Power Sources. 185 (2008) 1293–1304. doi:10.1016/j.jpowsour.2008.08.010.
- [4] P.D. Vaidya, A.E. Rodrigues, Insight into steam reforming of ethanol to produce hydrogen for fuel cells, Chemical Engineering Journal. 117 (2006) 39–49. doi:10.1016/j.cej.2005.12.008.
- [5] A. Haryanto, S. Fernando, N. Murali, S. Adhikari, Current Status of Hydrogen Production Techniques by Steam Reforming of Ethanol: A Review, ENERGY & FUELS. (2005) 2098–2106.



- [6] M. Ni, D.Y.C. Leung, M.K.H. Leung, A review on reforming bio-ethanol for hydrogen production, *International Journal of Hydrogen Energy*. 32 (2007) 3238–3247. doi:10.1016/j.ijhydene.2007.04.038.
- [7] E.T. Jordi Llorca, Vicente Cortés Corberán, Núria J. Divins, Raquel Olivera Fraile, Hydrogen from bio-ethanol, in: D. Gandía LM, Arzamendi G, E. PM (Eds.), *Renewable Hydrogen Technologies*, Elsevier, Amsterdam, 2013. doi:10.1016/B978-0-444-56352-1.00007-6.
- [8] J.L. Contreras, J. Salmones, J. a. Colín-Luna, L. Nuño, B. Quintana, I. Córdova, et al., Catalysts for H<sub>2</sub> production using the ethanol steam reforming (a review), *International Journal of Hydrogen Energy*. 39 (2014) 18835–18853. doi:10.1016/j.ijhydene.2014.08.072.
- [9] E. Lopez, V. Gepert, A. Gritsch, U. Nieken, G. Eigenberger, Ethanol Steam Reforming Thermally Coupled with Fuel Combustion in a Parallel Plate Reactor, *Industrial & Engineering Chemistry Research*. 51 (2012) 4143–4151. doi:10.1021/ie202364y.
- [10] H. Idriss, M. Scott, J. Llorca, S.C. Chan, W. Chiu, P.-Y. Sheng, et al., A phenomenological study of the metal-oxide interface: the role of catalysis in hydrogen production from renewable resources., *ChemSusChem*. 1 (2008) 905–10. doi:10.1002/cssc.200800196.
- [11] M. Domínguez, E. Taboada, E. Molins, J. Llorca, Ethanol steam reforming at very low temperature over cobalt talc in a membrane reactor, *Catalysis Today*. 193 (2012) 101–106. doi:10.1016/j.cattod.2012.02.004.
- [12] A. Basile, Hydrogen Production Using Pd-based Membrane Reactors for Fuel Cells, *Topics in Catalysis*. 51 (2008) 107–122. doi:10.1007/s11244-008-9128-6.
- [13] D. Mendes, S. Tosti, F. Borgognoni, A. Mendes, L.M. Madeira, Integrated analysis of a membrane-based process for hydrogen production from ethanol steam reforming, *Catalysis Today*. 156 (2010) 107–117. doi:10.1016/j.cattod.2010.02.029.
- [14] S. Tosti, A. Basile, L. Bettinali, F. Borgognoni, F. Gallucci, C. Rizzello, Design and process study of Pd membrane reactors, *International Journal of Hydrogen Energy*. 33 (2008) 5098–5105. doi:10.1016/j.ijhydene.2008.05.031.
- [15] F. Gallucci, A. Basile, Pd–Ag membrane reactor for steam reforming reactions: A comparison between different fuels, *International Journal of Hydrogen Energy*. 33 (2008) 1671–1687. doi:10.1016/j.ijhydene.2008.01.010.
- [16] M.M. Adrian bejan, George Tsatsarnois, *Thermal Design and optimization.pdf*, John Wiley, New York, USA, 1996.
- [17] N. Sato, *Chemical Energy and Exergy*, Elsevier Science & Technology Books, Amsterdam, 2004.
- [18] Y. Casas-Ledón, L.E. Arteaga-Perez, M.C. Morales-Perez, L.M. Peralta-Suárez, Thermodynamic Analysis of the Hydrogen Production from Ethanol: First and Second Laws Approaches, *ISRN Thermodynamics*. 2012 (2012). doi:10.5402/2012/672691.
- [19] Z. Khila, N. Hajjaji, M.-N. Pons, V. Renaudin, A. Houas, A comparative study on energetic and exergetic assessment of hydrogen production from bioethanol via steam reforming, partial oxidation and auto-thermal reforming processes, *Fuel Processing Technology*. 112 (2013) 19–27. doi:10.1016/j.fuproc.2013.02.013.

- [20] Y. Casas-Ledón, L.E. Arteaga-Perez, M.C. Morales-Perez, L.M. Peralta-Suárez, Thermodynamic Analysis of the Hydrogen Production from Ethanol: First and Second Laws Approaches, *ISRN Thermodynamics*. 2012 (2012) 1–8. doi:10.5402/2012/672691.
- [21] Y. Kalinci, A. Hepbasli, I. Dincer, Efficiency assessment of an integrated gasifier/boiler system for hydrogen production with different biomass types, *International Journal of Hydrogen Energy*. 35 (2010) 4991–5000. doi:10.1016/j.ijhydene.2009.08.079.
- [22] A. Modarresi, W. Wukovits, A. Friedl, Application of exergy balances for evaluation of process configurations for biological hydrogen production, *Applied Thermal Engineering*. 30 (2010) 70–76. doi:10.1016/j.applthermaleng.2009.04.027.
- [23] M. Orhan, I. Dincer, M. Rosen, Energy and exergy assessments of the hydrogen production step of a copper–chlorine thermochemical water splitting cycle driven by nuclear-based heat, *International Journal of Hydrogen Energy*. 33 (2008) 6456–6466. doi:10.1016/j.ijhydene.2008.08.035.
- [24] A.S. Joshi, I. Dincer, B. V. Reddy, Exergetic assessment of solar hydrogen production methods, *International Journal of Hydrogen Energy*. 35 (2010) 4901–4908. doi:10.1016/j.ijhydene.2009.09.067.
- [25] P. Tippawan, A. Arpornwichanop, Energy and exergy analysis of an ethanol reforming process for solid oxide fuel cell applications., *Bioresource Technology*. 157 (2014) 231–9. doi:10.1016/j.biortech.2014.01.113.
- [26] A. Hedayati, O. Le Corre, B. Lacarrière, J. Llorca, Exergetic study of catalytic steam reforming of bio-ethanol over Pd–Rh/CeO<sub>2</sub> with hydrogen purification in a membrane reactor, *International Journal of Hydrogen Energy*. IN PRESS (2014). doi:10.1016/j.ijhydene.2014.09.016.
- [27] E. López, N.J. Divins, J. Llorca, Hydrogen production from ethanol over Pd–Rh/CeO<sub>2</sub> with a metallic membrane reactor, *Catalysis Today*. 193 (2012) 145–150. doi:10.1016/j.cattod.2012.06.030.
- [28] R. Koch, E. López, N.J. Divins, M. Allué, A. Jossen, J. Riera, et al., Ethanol catalytic membrane reformer for direct PEM FC feeding, *International Journal of Hydrogen Energy*. 38 (2013) 5605–5615. doi:10.1016/j.ijhydene.2013.02.107.
- [29] M.K. Cohce, I. Dincer, M. a Rosen, Energy and exergy analyses of a biomass-based hydrogen production system., *Bioresource Technology*. 102 (2011) 8466–74. doi:10.1016/j.biortech.2011.06.020.
- [30] A.P. Hinderink, F.P.J.M. Kerkhof, A.B.K. Lie, J. De Swaan Arons, H.J. Van Der Kooi, Exergy analysis with a flowsheeting simulator—I. Theory; calculating exergies of material streams, *Chemical Engineering Science*. 51 (1996) 4693–4700. doi:10.1016/0009-2509(96)00220-5.
- [31] NASA polynomials, University of California, Berkeley. (n.d.). [http://www.me.berkeley.edu/gri-mech/data/nasa\\_plnm.html](http://www.me.berkeley.edu/gri-mech/data/nasa_plnm.html).
- [32] G.D. R. J. Kee, F. M. Rupley, J. A. Miller, M. E. Coltrin, J. F. Grcar, E. Meeks, H. K. Moffat, A. E. Lutz, W.C.R. M. D. Smooke, J. Warnatz, G. H. Evans, R. S. Larson, R. E. Mitchell, L. R. Petzold, and O.A. M. Caracotsios, W. E. Stewart, P. Glarborg, C. Wang, *Chemkin Thermodynamic Database, Reaction Design, San Diego, CA, 2000*.

- [33] N.J. Divins, E. López, Á. Rodríguez, D. Vega, J. Llorca, Bio-ethanol steam reforming and autothermal reforming in 3- $\mu\text{m}$  channels coated with RhPd/CeO<sub>2</sub> for hydrogen generation, *Chemical Engineering and Processing: Process Intensification*. 64 (2013) 31–37. doi:10.1016/j.cep.2012.10.018.